Analytical Dynamics in Rotating Frames

Kanter Iris under the supervision of Dr. Martinusi Vladimir

May 30, 2024

Abstract

This research study examines the two-point boundary value problem as outlined by Kepler (unperturbed), applied to scenarios involving both rotating and non-rotating earth, focusing on the path of least energy consumption. For the scenario considering a non-rotating earth, a solution is derived analytically, leveraging the symmetry inherent to the problem. In contrast, for the rotating earth scenario, the approach adopts a numerical strategy, specifically the fixed-point iteration (FPI) method, starting with the solution for the non-rotating case as the initial guess. The results of this method manifests in behaviors akin to first or second-order responses, which is elucidated through the examination of the relationship between angular distance and Time of Flight (ToF). We present an exponential convergence rate fitting of the miss distance for FPI.

1 Preliminaries

1.1 Kepler's Problem

This section presents a qualitative approach to Kepler's problem, which models the trajectory of a point of mass m orbiting under the gravitational influence of another point of mass M, such that $m << M$. The mathematical model of the Kepler's problem (represented in an inertial frame of reference) is:

$$\ddot{\mathbf{r}} + \frac{\mu}{r^3}\mathbf{r} = \mathbf{0},\ \mathbf{r}\left(t_0\right) = \mathbf{r}_0,\ \dot{\mathbf{r}}\left(t_0\right) = \mathbf{v}_0 \tag{1}$$

where $\mu = GM$ is the standard gravitational parameter. Here G stands for Newton's universal gravitational constant.

1.1.1 Constants of Motion in Kepler's Problem

The specific energy is derived by dot-multiplying Equation (1) with the velocity vector $\mathbf{v}$ and utilizing the relationship $\dot{r} = \frac{\mathbf{v}\cdot\mathbf{r}}{r}, \dot{\mathbf{r}} \equiv \mathbf{v}$:

$$\varepsilon = \frac{\mathbf{v}^2}{2} - \frac{\mu}{r} = \frac{\mathbf{v}_0^2}{2} - \frac{\mu}{r_0} \tag{2}$$

The specific angular momentum is obtained by taking the cross product of equation (1) with the position vector $\mathbf{r}$:

$$\mathbf{h} = \mathbf{r} \times \mathbf{v} = \mathbf{r}_0 \times \mathbf{v}_0 \tag{3}$$

The Laplace-Runge-Lenz vector is found by differentiating the normalized position vector $\frac{\mathbf{r}}{r}$:

$$\mu\mathbf{e} = \mathbf{v} \times \mathbf{h} - \mu\frac{\mathbf{r}}{r} = \mathbf{v}_0 \times (\mathbf{r}_0 \times \mathbf{v}_0) - \mu\frac{\mathbf{r}_0}{r_0} \tag{4}$$

The conservation of angular momentum implies that the motion takes place in a fixed plane. More specifically, on a conic section, whose polar equation can be deduced from:

$$\mathbf{e} \cdot \mathbf{r} + r = p \equiv \frac{\mathbf{h}^2}{\mu} \tag{5}$$

$$r = \frac{p}{1 + e\cos f}, f \triangleq \angle(\mathbf{r}, \mathbf{e}) \tag{6}$$

In the elliptic case, the periapsis and apoapsis, representing the minimum and maximum values of the radial distance r, are defined as follows:

$$r_p = r_{\min} = \frac{p}{1+e} \tag{7}$$

$$r_a = r_{\max} = \frac{p}{1-e} \tag{8}$$

The semimajor axis is:

$$a = \frac{r_a + r_p}{2} = \frac{p}{1-e^2} \tag{9}$$

The conserved energy is evaluated at the periapsis, where the velocity is perpendicular to the position vector:

$$\mathbf{h}^2 = (\mathbf{r}_p \times \mathbf{v}_p) \cdot (\mathbf{r}_p \times \mathbf{v}_p) = \mathbf{v}_p^2 \mathbf{r}_p^2 \tag{10}$$

Similarly, the relationship between the specific energy ε and the semimajor axis, in the elliptical case, is derived as:

$$\varepsilon = \frac{\mathbf{v}_p^2}{2} - \frac{\mu}{r_p} = \frac{h^2}{2r_p^2} - \frac{\mu}{r_p} \tag{11}$$

$$= \frac{\mu}{r_p}\left(\frac{p}{2r_p} - 1\right) \tag{12}$$

$$= \frac{\mu}{2r_p}(e-1) = -\frac{\mu}{2a} \tag{13}$$

1.1.2 Kepler's Time Equation

For elliptical orbits, the eccentric anomaly E is defined as:

$$\cos E = \frac{e + \cos f}{1 + e\cos f};\ \sin E = \frac{\sqrt{1-e^2}\sin f}{1 + e\cos f} \tag{14}$$

This implies that the radial distance r can be expressed with respect to the eccentric anomaly as:

$$r = a\left(1 - e\cos E\right) \tag{15}$$

while the differential of the eccentric anomaly satisfies:

$$rdE = a\sqrt{\frac{\mu}{a^3}}dt \triangleq na \cdot dt \tag{16}$$

From the latter:

$$\Delta t = \frac{1}{n}\int \left(1 - e\cos E\right) dE = \frac{\Delta\left(E - e\sin\left(E\right)\right)}{n} \triangleq \frac{\Delta M}{n} \tag{17}$$

1.2 The Velocity Hodograph

From [Condurache, 2007] we can isolate the velocity in terms of $\mathbf{h}, \mathbf{r}, \mathbf{e}$ by taking the cross product of equation (4) with $\mathbf{h}$:

$$\mathbf{h}\times\mathbf{e} = \mathbf{h}\times\left(\frac{\mathbf{v}\times\mathbf{h}}{\mu}\right) - \mathbf{h}\times\frac{\mathbf{r}}{r} = \frac{h^2}{\mu}\mathbf{v} - \mathbf{h}\times\frac{\mathbf{r}}{r} \tag{18}$$

$$\mathbf{v} = \frac{h}{p}\left(\frac{\mathbf{h}}{h}\times\mathbf{e} + \frac{\mathbf{h}}{h}\times\frac{\mathbf{r}}{r}\right) \tag{19}$$

Thus, the velocity vector consists of two components: a constant and a rotating component.

1.3 Rodrigues' Rotation Formula (Lie groups derivation)

Claim 1.3.1 *a rotation of* $\mathbf{v}$ *around unitary vector* u *with angle* α *(i.e. an orthogonal operator* $\mathbf{R} \in \left\{\mathbb{M}^3, \mathbf{R}^T\mathbf{R} = \mathbb{I}\right\} = SO_n$*) can be represented as:*

$$\mathbf{R}\left(\alpha, \mathbf{u}\right) = \mathbb{I} + \sin\left(\alpha\right)\mathbf{u} + \left(1 - \cos\left(\alpha\right)\right)\widetilde{u}^2 \tag{20}$$

Where:

$$\widetilde{u} = \begin{bmatrix} 0 & -u_3 & u_2 \\ u_3 & 0 & -u_1 \\ -u_2 & \omega_1 & 0 \end{bmatrix} \tag{21}$$

Proof. From [Murray, 1994]

$$\exp\left(\widetilde{\boldsymbol{\omega}}\right) \in SO_n \tag{22}$$

$$\exp\left(\widetilde{\boldsymbol{\omega}}\right) = \mathbb{I} + \widetilde{\boldsymbol{\omega}} + \frac{\widetilde{\boldsymbol{\omega}}^2}{2} + ... \tag{23}$$

In the 3D case:

$$\widetilde{\boldsymbol{\omega}}^2 = -\omega^2 \widetilde{\boldsymbol{\omega}} \tag{24}$$

so equation (23) becomes:

$$\begin{aligned} \exp\left(\widetilde{\boldsymbol{\omega}}\right) &= \mathbb{I} - \left(\frac{\omega^2}{2} + \frac{\omega^3}{6}...\right)\widetilde{\boldsymbol{\omega}} && (25) \\ &= \mathbb{I} + \sin\omega\frac{\widetilde{\boldsymbol{\omega}}}{\omega} + (1-\cos\omega)\frac{\widetilde{\boldsymbol{\omega}}}{\omega} \triangleq \mathbf{R}\left(\alpha, \mathbf{u}\right) && (26) \end{aligned}$$

■

2 Results

In this section, we will present solutions for Kepler's boundary value problem. The first solution is an analytical one for the non-rotating earth case, while the second solution consists of numerical results obtained for a rotating earth. Both solutions operate under the constraint of minimal energy elliptic trajectory. Only gravitational forces are modeled, with atmospheric drag, J2, and other perturbations being ignored.
We also note, that the results assume an orthonormal inertial frame of reference (with the origin located at the center of the earth) and that the Dirichlet's boundary conditions for Kepler's problem, denoted by $\mathbf{A}$ (launch) and $\mathbf{B}$ (target), satisfy being equidistant (R) from the center of the earth.

2.1 Analytical Solution (non-rotating Earth)

The result is obtained by utilizing the symmetry of the problem. A key scalar parameter governing the problem, as we will presently present, is the angular distance between the boundaries $\mathbf{A}, \mathbf{B}$:

$$2\gamma = \arccos(\frac{\mathbf{A}\cdot\mathbf{B}}{R^2}), \gamma \in \left(0, \frac{\pi}{2}\right) \tag{27}$$

since $\mathbf{A}, \mathbf{B}$ span the plane of motion (assuming they are not co-linear, i.e. not a self-launch):

$$\frac{\mathbf{h}}{h} = \frac{\mathbf{A}\times\mathbf{B}}{||\mathbf{A}\times\mathbf{B}||} \tag{28}$$

From (11) and (7), for the elliptic case ($0 < e < 1$, $\varepsilon < 0$) we have the relations:

$$p = r\left(1 + e\cdot\cos(f)\right) = R\left(1 + e\cdot\cos(f_{\mathbf{A/B}})\right) \tag{29}$$

$$\varepsilon_{\min} \iff a_{\min} \tag{30}$$

Employing the Euclidean metric and denoting $\mathbf{F}$ as the second foci of the ellipse (the first being at the center of the earth) results in:

$$\begin{aligned} d(\mathbf{A},\mathbf{0}) + d(\mathbf{A},\mathbf{F}) &= d(\mathbf{B},\mathbf{0}) + d(\mathbf{B},\mathbf{F}) && (31) \\ d(\mathbf{A},\mathbf{F}) &= d(\mathbf{B},\mathbf{F}) && (32) \end{aligned}$$

The latter symmetry implies that point $\mathbf{F}$ lies on the angle bisector of $\angle(\mathbf{A}, \mathbf{0}, \mathbf{B})$. Since $\mathbf{F}$ is collinear with the eccentricity vector $\mathbf{e}$, we can leverage this symmetry to partition the solution into two cases based on the direction of the eccentricity vector:

$$\frac{\mathbf{e}}{e} = \pm \frac{\mathbf{A} + \mathbf{B}}{||\mathbf{A} + \mathbf{B}||} \tag{33}$$

2.1.1 Cases Study

Case 2.1.1

$$\frac{\mathbf{e}}{e} = -\frac{\mathbf{A} + \mathbf{B}}{||\mathbf{A} + \mathbf{B}||} \tag{34}$$

$$f_A = \pi - \gamma, f_B = \pi + \gamma \tag{35}$$

From (29):

$$p = R\left(1 - e\cos\left(\gamma\right)\right) \tag{36}$$

$$a = \frac{R\left(1 - e\cos\left(\gamma\right)\right)}{1 - e^2} \tag{37}$$

Since γ is known, we have obtained $a = a(e)$. Differentiating to find the minimal energy trajectory using Ferma's Theorem:

$$\frac{da(e)}{de} = \frac{-R\left(1 - e^2\right)\cos\left(\gamma\right) + 2eR\left(1 - e\cos\left(\gamma\right)\right)}{(1 - e^2)^2} \tag{38}$$

$$0 = \left(\cos\left(\gamma\right)\right)e^2 - 2e + \cos\left(\gamma\right) \tag{39}$$

$$e_{1,2} = \frac{1}{\cos\left(\gamma\right)} \pm \sqrt{\frac{1}{\cos^2\left(\gamma\right)} - 1} \tag{40}$$

$$e_{\min \varepsilon}(\gamma) = \frac{1}{\cos\left(\gamma\right)} - \sqrt{\frac{1}{\cos^2\left(\gamma\right)} - 1} = \frac{1 - \sin(\gamma)}{\cos\left(\gamma\right)} \tag{41}$$

We can see that the solution is governed by the value of γ, and is decreasing as γ reaches it upper limit $(\frac{\pi}{2})$.Using the second derivative test, one can verify that this is indeed a local minimum.

Case 2.1.2 *repeating a similar process*

$$\frac{\mathbf{e}}{e} = \frac{\mathbf{A} + \mathbf{B}}{||\mathbf{A} + \mathbf{B}||} \tag{42}$$

$$f_A = 2\pi - \gamma, f_B = \gamma \tag{43}$$

$$a = \frac{R\left(1 + e \cdot \cos(\gamma)\right)}{1 - e^2} \tag{44}$$

$$e_{1,2} = \text{-}\frac{1}{\cos\left(\gamma\right)} \mp \sqrt{\frac{1}{\cos^2\left(\gamma\right)} - 1} \tag{45}$$

The latter indicates that the two cases coincide.

2.1.2 Outcome IC's

We previously presented the solution for $e_{\min\varepsilon}(\gamma)$, which, settles the minimal energy ellipse for the given boundaries. We now proceed in deriving the IC's (i.e. the velocity required at the launch point, $\mathbf{A}$)

$$\mathbf{e}_{\min\varepsilon}(\mathbf{A},\mathbf{B}) = e_{\min\varepsilon}\frac{\mathbf{A}+\mathbf{B}}{||\mathbf{A}+\mathbf{B}||} \tag{46}$$

$$p_{\min\varepsilon}(\mathbf{A},\mathbf{B}) = R\left(1 - e_{\min\varepsilon}\cos\gamma\right) \tag{47}$$

$$h_{\min\varepsilon}(\mathbf{A},\mathbf{B}) = \sqrt{\mu p_{\min\varepsilon}}\frac{\mathbf{A}\times\mathbf{B}}{||\mathbf{A}\times\mathbf{B}||} \tag{48}$$

$$\mathbf{v}_{A\,\min\varepsilon}(\mathbf{A},\mathbf{B}) = \frac{h_{\min\varepsilon}}{p_{\min\varepsilon}}\left(\frac{\mathbf{h}_{\min\varepsilon}}{h_{\min\varepsilon}}\times\mathbf{e}_{\min\varepsilon} + \frac{\mathbf{h}_{\min\varepsilon}}{h_{\min\varepsilon}}\times\frac{\mathbf{A}}{R}\right) \tag{49}$$

Remark 2.1.3 *Earths rotation is not deducted from the output velocity launch vector since the model is used outside the atmosphere (for example replace* $R[km]$ *with* $6371 + 100$ *for Kármán line).*

Time of flight calculation can also be simplified using the governed symmetry:

$$ToF_{A\to B_{\min\varepsilon}} = 2\Delta t_{A\to apoapsis} = \frac{2}{n_{\min\varepsilon}}\left[\pi - \left(E_A - e_{\min\varepsilon}\sin E_A\right)\right] \tag{50}$$

$$F(\gamma) \triangleq \frac{\sqrt{1-\mathbf{e}^2_{\min\varepsilon}}\sin\gamma}{\mathbf{e}_{\min\varepsilon} - \cos\gamma} \tag{51}$$

$$ToF(\gamma) = \frac{2}{n_{(\gamma)}}\left[\pi - \arctan\left(F(\gamma)\right) + \mathbf{e}(\gamma)\sin\left(\arctan\left(F(\gamma)\right)\right)\right] \tag{52}$$

2.2 Numerical Results for Rotating Earth

When dealing with 1D root-finding problems, where the root is also a local minimum, traditional root-finding methods like Newton's method may not perform optimally. Hence, a numerical fixed point iteration method was chosen.
Consider the earth's rotation and utilizing the analytical solution previously found as the initial guess. The problem is redefined as follows:

Problem 2.2.1 *which aiming point* $\mathbf{B}^{(n)}$ *will result in hitting* $\mathbf{B}$ *at* $t = ToF_{\mathbf{A}\to\mathbf{B}^{(n)}_{\min\ \varepsilon}}$*?*

Where $\mathbf{B}^{(n)}$ is defined as:

$$\mathbf{B}^{(n)} = \mathbf{R}\left(\omega \cdot ToF_{\mathbf{A}\to\mathbf{B}^{(n-1)}_{\min\ \varepsilon}}, \frac{\boldsymbol{\omega}}{\omega}\right)\mathbf{B}, n = 1, ... \tag{53}$$

$\boldsymbol{\omega}$ is earth's rotation axis, $|\boldsymbol{\omega}| = \omega$ is earth's rotation rate and $ToF_{\mathbf{A}\to\mathbf{B}^{(0)}_{\min\ \varepsilon}}$ stands for the analytical non-rotating solution given by $\mathbf{A}, \mathbf{B}$.
Since $\frac{2\pi}{\omega} >> ToF$ we expect the solution to be in the vicinity of the solution (and eastward to $\mathbf{B} = \mathbf{B}^{(0)}$). After convergence is achieved the Analytical results as described in (46) for $\mathbf{B}^{(n)}$ are returned to the user.

Remark 2.2.2 *The frame of reference that is utilized in the code is ECEF which is a non inertial since it rotates with the earth. The reason that it is possible to use it, is that we assumed for the analytical part, a non-rotating frame of reference. Hence, the outputted minimal velocity vector is in ECEF coordinates.*

Remark 2.2.3 *The method's stopping conditions is about the miss (angular) distance $\Delta^{(n)}$ between the aiming point $\mathbf{B}^{(n)}$ and the target at time of hit $\mathbf{B}^{(n-1)}$:*

$$\Delta^{(n)} = \arccos\left(\frac{\mathbf{B}^{(n)}\cdot\mathbf{B}^{(n-1)}}{R^2}\right) < \delta \tag{54}$$

2.3 Method's behaviour

In this section we present graphs of 2 representing cases: each for targeting a coordinate that is either west/east relative to launch point $\mathbf{A}$.

The results are for launch coordinates in GCS $\begin{bmatrix} R\ [km] \\ \text{longitude} \circ \text{deg} \\ \text{latitude} \circ \text{deg} \end{bmatrix}$:

$$\begin{bmatrix} 6371 + 100 \\ 30.997569 \circ \text{deg} \\ 35.142919 \circ \text{deg} \end{bmatrix} \text{Launch (Dimona)} \tag{55}$$

$$\begin{bmatrix} 6371 + 100 \\ 51.695562 \circ \text{deg} \\ 32.621066 \circ \text{deg} \end{bmatrix} \text{East target (Isfahan)} \tag{56}$$

$$\begin{bmatrix} 6371 + 100 \\ 16.596731 \circ \text{deg} \\ 31.063835 \circ \text{deg} \end{bmatrix} \text{West target (Lybia)} \tag{57}$$

With $1[m]$ allowed of miss distance and $10^{-5}[rad]$ meshing resolution (used for validation of the method as we will presently explain).

2.3.1 ToF-γ relation

To presently explain the method's behaviour, see appendix A for $\frac{dTof(\gamma)}{d\gamma} > 0$ proof.

2.3.2 'East' Targets (Relative to A and ω)

For aiming point that are east relative to launch point and axis of rotation (since for earth, axis of rotation is **z**, 'east' receives it's nominal interpretation):

$$\gamma^{(1)} > \gamma^{(0)} \Rightarrow ToF^{(1)} > ToF^{(0)} \Rightarrow \tag{58}$$

$$\gamma^{(2)} > \gamma^{(1)} \Rightarrow ... \Rightarrow \gamma \text{ and } ToF \text{ both increase until convergence} \tag{59}$$

$$\Rightarrow \text{Convergence exhibit a first-order response behaviour} \tag{60}$$

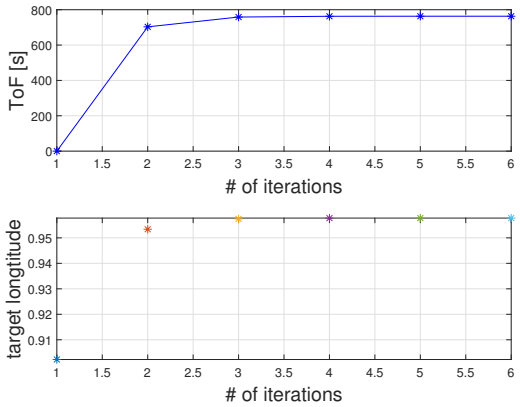

Figure 1: Temporal first order response (upper), spatial first order response (lower)

2.3.3 'West' Targets (Relative to A and ω)

Similarly, for aiming points to that are west relative to launch point and axis of rotation :

$$\gamma^{(1)} < \gamma^{(0)} \Rightarrow ToF^{(1)} < ToF^{(0)} \Rightarrow \tag{61}$$

$$\Rightarrow \gamma^{(2)} > \gamma^{(1)} \Rightarrow ... \Rightarrow \gamma \text{ and } ToF \text{ both oscillates until convergence} \tag{62}$$

$$\Rightarrow \text{Convergence exhibit a second-order response behaviour} \tag{63}$$

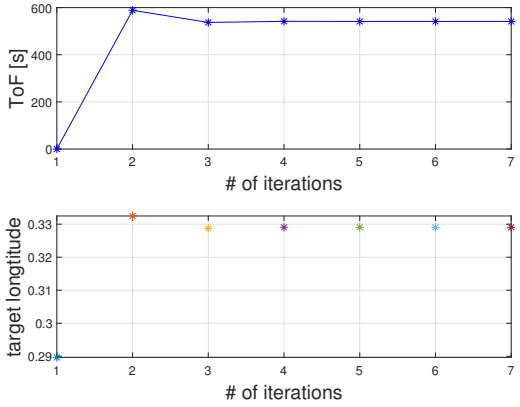

Figure 2: Temporal second order response (upper), spatial second order response (lower)

2.3.4 Poles and 'Self-Aim'

If the target is at the poles of the rotation axis it will not move relative to the aiming point at t=0. Hence, the code will converge from the first iteration.

Remark 2.3.1 *Self aim* ($\mathbf{A} = \mathbf{B}$) *results in* $e = 1$ *and the numerical method will fail.*

Remark 2.3.2 *For equality in longitude or latitude (but not for both, i.e. not a self-aim) the 'East' and 'West' behaviour applies.*

2.3.5 Convergence Rate

The method exhibits an exponential convergence rate

$$\Delta^{(n)} = \Delta^{(1)} e^{-2.5(n-1)} \ [rad] \tag{64}$$

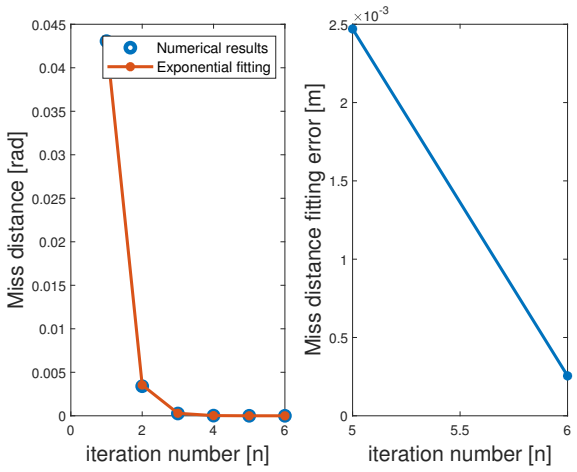

Figure 3: Eastern target: Miss distance fitting (left), fitting error (right)

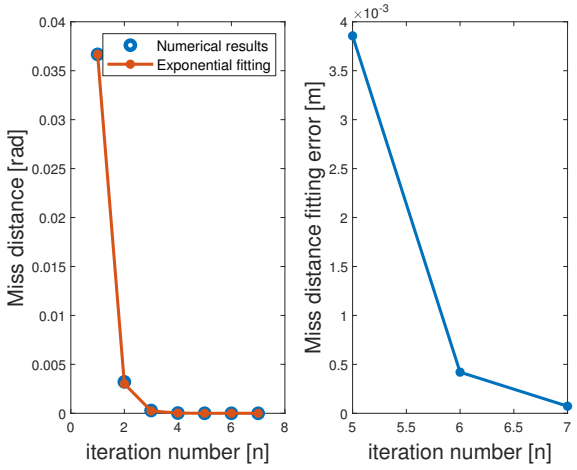

Figure 4: Western target: Miss distance fitting (left), fitting error(right)

2.3.6 Verifying Numerical Results

meshing the circular curve, on which the target is moving, to central angles, and calculating the miss distance when aiming to each node is one of the way to verify that the numerical method indeed converges to the desired value.

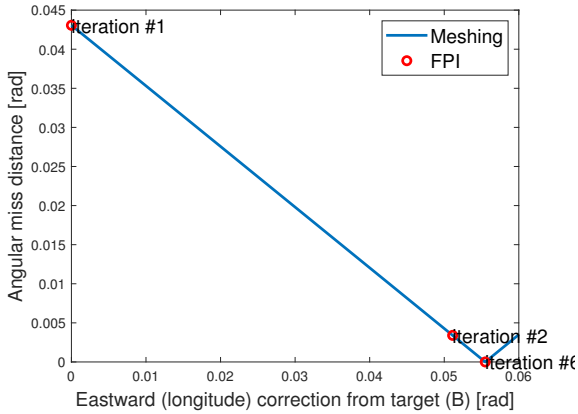

Figure 5: Eastern target: FPI mesh verification (upper), A closer look (lower)

Also, the sensitivity of numerical parameters such as meshing resolution and stopping conditions was examined (see appendix B).

3 Conclusions

- An analytical solution for non-rotating classic Kepler's boundary value problem is achieved using symmetry.
- The angular distance between the boundaries (γ) is the scalar that dominates the analytical solution.
- Investigating the dissection into two topological loci (east and west), we find

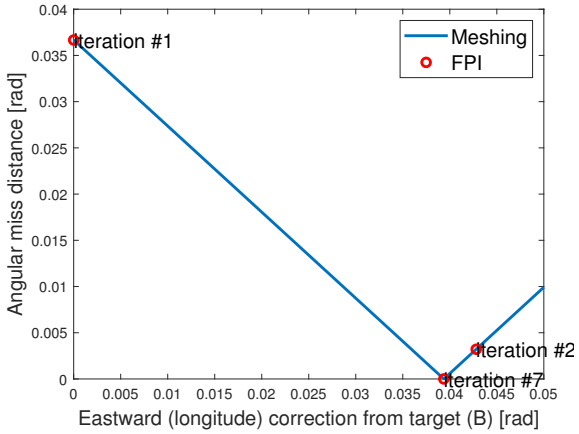

Figure 6: Western target: FPI mesh verification (upper), A closer look (lower)

that the suggested convergence behavior exhibits similarities to first and second-order responses which arises due $\frac{dTof(\gamma)}{d\gamma} > 0$.

- FPI numerical method is converging exponentially.
- Further research suggested is exploring Banach fixed-point theorem and the notion of attracting fixed points, to shed more light on the convergence rate obtained, and whether or not the method's convergence is assured regardless to the initial guess (e.g. a slow rotation of the planet relative to ToF is a requirement for convergence).

References

[Condurache, 2007] Condurache, M. (2007). A short solution to the keplerian ballistic problem using the velocity hodograph. *Bul. Inst. Polit. Iasi,Sect. Mathematics, Theoretical Mechanics, Physics.*

[Murray, 1994] Murray, R.M., L. Z. . S. S. (1994). A mathematical introduction to robotic manipulation (1st ed.). *CRC Press.*

4 Appendix A

$$ToF = \frac{2}{n}\left[\pi - E_{\mathbf{A}} + e\sin E_{\mathbf{A}}\right] \tag{65}$$

Where $E_{\mathbf{A}}$ is corresponding to the true anomaly of $\mathbf{A}$.

$$\frac{dToF}{d\gamma} = \frac{dToF}{dn}\frac{dn}{d\gamma} + \frac{dToF}{dE_{\mathbf{A}}}\frac{dE_{\mathbf{A}}}{d\gamma} + \frac{dToF}{de}\frac{de}{d\gamma} \tag{66}$$

$$\frac{dToF}{dn}\frac{dn}{d\gamma} = -\frac{6\cos\gamma - \sin\gamma + 1)\sqrt{2mu}(e\sin E - E + \pi)}{R^{3/2}\sqrt{\sin\gamma + 1}(\cos\gamma^2 + (-\sin\gamma - 1)\cos\gamma - 2\sin\gamma - 2)n^2} > 0 \tag{67}$$

$$\frac{dToF}{dE_{\mathbf{A}}}\frac{dE_{\mathbf{A}}}{d\gamma} = \frac{\sqrt{2}}{n\sqrt{\sin\gamma + (\sin\gamma)^2}} > 0 \tag{68}$$

$$\frac{dToF}{de}\frac{de}{d\gamma} = \frac{-2\sin E_{\mathbf{A}}}{n(\sin\gamma + 1)} < 0 \tag{69}$$

Even though that the latter is negative, it can be verified that:

$$\frac{dToF}{dE_{\mathbf{A}}}\frac{dE_{\mathbf{A}}}{d\gamma} - \frac{dToF}{de}\frac{de}{d\gamma} > 0 \tag{70}$$

■

5 Appendix B

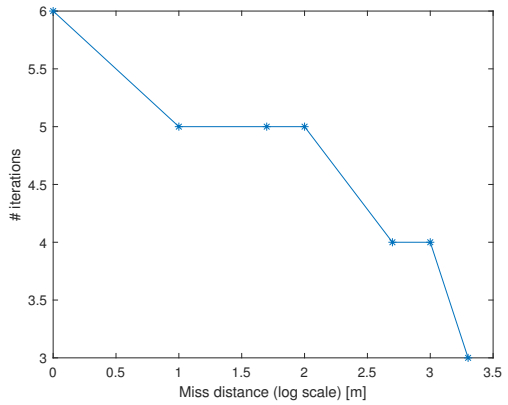

Figure 7: Eastern target: miss distance analysis

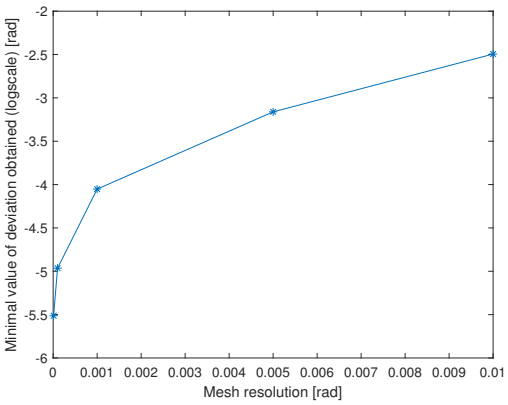

Figure 8: Eastern target: mesh resolution convergence graph

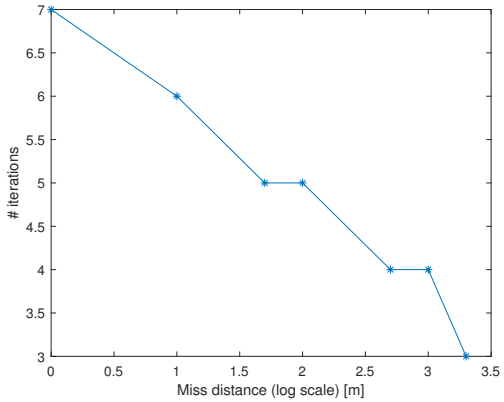

Figure 9: Western target: miss distance analysis

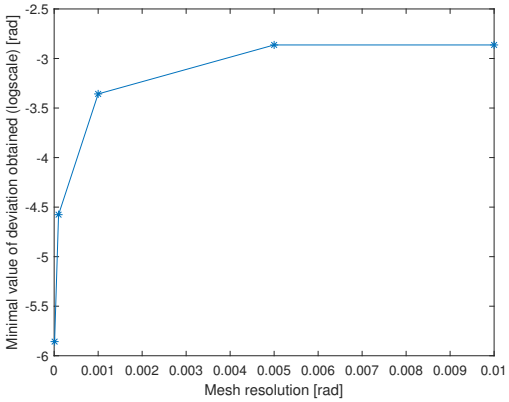

Figure 10: Western target: mesh resolution convergence graph